JOURNAL OF AGRICULTURAL AND FOOD CHEMISTRY

Article

pubs.acs.org/JAFC

Synthesis and Evaluation of Heterocyclic Analogues of Bromoxynil

Matthew A. Cutulle,*[,†,¶] Gregory R. Armel,[†] James T. Brosnan,[†] Michael D. Best,[‡] Dean A. Kopsell,[†] Barry D. Bruce,[#] Heidi E. Bostic,[§] and Donovan S. Layton[⊥]

[†]Department of Plant Sciences, University of Tennessee, Knoxville, Tennessee 37996, United States

[‡]Department of Chemistry, University of Tennessee, Knoxville, Tennessee 37996, United States

[#]Department of Biochemistry Cell Biology and Molecular Biology, University of Tennessee, Knoxville, Tennessee 37996, United States

[§]Department of Chemistry, Wofford College, Spartanburg, South Carolina 29303, United States

[⊥]Department of Chemical and Biomolecular Engineering, University of Tennessee, Knoxville, Tennessee 37996, United States

ABSTRACT: One attractive strategy to discover more active and/or crop-selective herbicides is to make structural changes to currently registered compounds. This strategy is especially appealing for those compounds with limited herbicide resistance and whose chemistry is accompanied with transgenic tools to enable herbicide tolerance in crop plants. Bromoxynil is a photosystem II (PSII) inhibitor registered for control of broadleaf weeds in several agronomic and specialty crops. Recently at the University of Tennessee—Knoxville several analogues of bromoxynil were synthesized including a previously synthesized pyridine (2,6-dibromo-5-hydroxypyridine-2-carbonitrile sodium salt), a novel pyrimidine (4,6-dibromo-5-hydroxypyrimidine-2-carbonitrile sodium salt), and a novel pyridine *N*-oxide (2,6-dibromo-1-oxidopyridin-1-ium-4-carbonitrile). These new analogues of bromoxynil were also evaluated for their herbicidal activity on soybean (*Glycine max*), cotton (*Gossypium hirsutum*), redroot pigweed (*Amaranthus retroflexus*), velvetleaf (*Abutilon theophrasti*), large crabgrass (*Digitaria sanguinalis*), and pitted morningglory (*Ipomoea lacunose*) when applied at 0.28 kg ha^{-1}. A second study was conducted on a glyphosate-resistant weed (*Amaranthus palmeri*) with the compounds being applied at 0.56 kg ha^{-1}. Although all compounds were believed to inhibit PSII by binding in the quinone binding pocket of D1, the pyridine and pyridine-*N*-oxide analogues were clearly more potent than bromoxynil on *Amaranthus retroflexus*. However, application of the pyrimidine herbicide resulted in the least injury to all species tested. These variations in efficacy were investigated using molecular docking simulations, which indicate that the pyridine analogue may form a stronger hydrogen bond in the pocket of the D1 protein than the original bromoxynil. A pyridine analogue was able to control the glyphosate-resistant *Amaranthus palmeri* with >80% efficacy. The pyridine analogues of bromoxynil showed potential to have a different weed control spectrum compared to bromoxynil. A pyridine analogue of bromoxynil synthesized in this research controlled several weed species greater than bromoxynil itself, potentially due to enhanced binding within the PSII binding pocket. Future research should compare this analogue to bromoxynil using optimized formulations at higher application rates.

KEYWORDS: *bromoxynil, herbicide resistance, glyphosate resistance, Palmer amaranth*

INTRODUCTION

No new herbicidal mode of action has been incorporated into weed management strategies in over 20 years.[1] Prior to 1991 a new mode of action was introduced to the market approximately every three years. The dearth of novel herbicidal modes of action has led to selection pressure for herbicide-resistant weed biotypes in many different cropping systems. Currently, over 400 weedy biotypes exist that are resistant to at least one herbicide active ingredient.[2] To that end, optimization of molecules with the potential to either provide new modes of action or target established sites where resistance is not problematic is important for the future of weed management.[3,4]

A known target site with the potential to be exploited further is the plastoquinone binding site (Q_B) of the photosystem II (PSII) reaction center. PSII consists of multiple protein subunits and acts as a water:quinol oxidoreductase in all oxygenic organisms including cyanobacteria, algae, and plants. Upon illumination, the reaction center primary donor P680 becomes excited to a singlet state, where it then rapidly undergoes charge separation. P680 chlorophyll donates an electron to a proximal pheophytin (Ph) molecule, which leads to the formation of a $P680^{\bullet+}Ph^{\bullet-}$ radical pair. The occurrence of the radical pair is brief, as an electron is transferred from the Ph anion to the nonmobile plastoquinone electron acceptor Q_A to form the $P680^{\bullet+}Q_A{}^{\bullet-}$ radical.[6,7] Subsequently, an electron is transferred to Q_B via several intermediates. $P680^+$ is then rereduced by extracting an electron from Tyr_{161} of the D1 protein, which leads to the formation of a $TyrZ^{\bullet}(H^+)Q_A{}^{\bullet}$ radical pair.[8,9] This cation is then stabilized by the Mn_4Ca cluster in the oxygen-evolving complex, which upon further illumination extracts four electrons from two H_2O molecules to evolve O_2. On the other side of the membrane the electron is transferred from Q_A to Q_B via the nonheme Fe. After accepting

Received: August 1, 2013
Revised: December 16, 2013
Accepted: December 19, 2013
Published: December 19, 2013

dx.doi.org/10.1021/jf404209d | *J. Agric. Food Chem.* 2014, 62, 329−336

two electrons Q_B is converted to plastoquinol and released from the D1 binding pocket.[5]

Generally, PSII-inhibiting herbicides bind at the exchangeable Q_B site of the D1 protein in the PSII reaction center.[10−14] Binding of these herbicides displaces plastoquinone at the Q_B site; thus, the less mobile Q_A is unable to be oxidized. This leads to a charge recombination pathway resulting in the formation of triple chlorophyll and singlet oxygen species, which causes lipid peroxidation and general oxidative stress.[5,15] However, PSII inhibitors can interact with different portions of this binding pocket of the D1 protein. On the basis of simulation modeling and D1 mutant studies, phenolic herbicides such as bromoxynil and ioxynil form hydrogen bonds with His_{215} in the D1 protein, whereas it is believed that triazines and ureas do not form a hydrogen bond at this residue; rather they form a hydrogen bond at Ser_{264} of the D1 protein.[16,17]

Currently, there are approximately 70 weedy biotypes that are resistant to triazine herbicides, and many of the biotypes contain a Ser to Gly_{264} mutation.[2,18] Comparatively, only one weedy biotype is resistant to phenolic herbicides, and the mechanism of resistance is metabolism based.[2] Also, weedy biotypes containing the Gly_{264} mutation are hypersensitive to phenolic herbicides.[19,20] Resistance to phenolic herbicides is less likely to occur for two reasons: (1) bromoxynil and ioxynil typically have limited residual soil activity when compared to triazine herbicides; thus, there is less selection pressure on the seed bank for resistant biotypes[21,22]; and (2) $Hist_{215}$ and three other histidine residues form hydrogen bonds with the nonheme iron. This amino acid residue is more conserved than Ser_{264}; thus, resistance is less likely to occur due to target site mutations.

Physiologically, the interaction of His_{215} with phenolic herbicides could be exploited further with analogues of different electronegative properties because of the proximity of phenolic herbicides to Q_A.[16] Essentially, a molecular bridge forms between Q_A, His_{214} of the D2 protein, the nonheme iron, His_{215} of the D1 protein, and Q_B. The CO group on bromoxynil, which is deprotonated at physiological pH, forms a stronger hydrogen bond with the NH imidazole group on His_{215} than plastoquinone.[16] The tighter bond coupled with slightly different electron density characteristics of the herbicide likely affects the conformation of the Q_A−His_{214}−iron−His_{215}−Q_B system. Specifically, the hydrogen bond strength of the Q_A CO group and the imidazole NH group off His_{214} is likely altered.[23] Subsequently, the redox potential of Q_A is reduced, which leads to a charge recombination that favors $P680^+pPheo^-$, ultimately leading to a triplet chlorophyll state. Evaluation of analogues of phenolic herbicides is warranted given how important the Q_A−His_{214}−iron−His_{215}−Q_B molecular bridge is in PSII. In particular, heterocyclic[24] analogues (cyclic structures containing atoms other than carbon) of the phenolic herbicides would be interesting candidates for evaluation because of the potential impact that a ring structure with different electronegative properties would have on the π electron system of the molecular bridge, Q_B binding site, and redox potential of Q_A.

Bromoxynil is an ideal phenolic PSII inhibitor for structural modification because of its current significance to the marketplace, limited environmental impact due to rapid degradation in the soil, and effectiveness when applied postemergence (POST) for control of many problematic broadleaf weeds including pitted morningglory.[25,26] Bromoxynil is labeled for use in alfalfa (*Medicago sativa*), cereals, corn (*Zea mays*), flax (*Linum usitatissimum*), mint (*Mentha spicata*), garlic (*Allium sativum*), and onions (*Allium cepa*).[22] Commercially, bromoxynil is formulated as an ester to help penetrate the hydrophobic cuticle of weeds. Subsequently, the herbicide is then hydrolyzed by plant enzymes to a free acid molecule.[27] Typically, bromoxynil absorption is greater in shoots than in roots because bromoxynil is conjugated in the soil and does not translocate as easily to leaves.[28,29]

An understanding of bromoxynil's impact on plant physiology, availability of the target crystal structure of the D1 protein, and bromoxynil's importance to weed management make bromoxynil an interesting compound for optimization. Research was conducted to evaluate novel heterocyclic analogues of bromoxynil synthesized on site for crop tolerance and weed control. Further analysis was performed by simulating the interaction of bromoxynil analogues in the binding pocket.

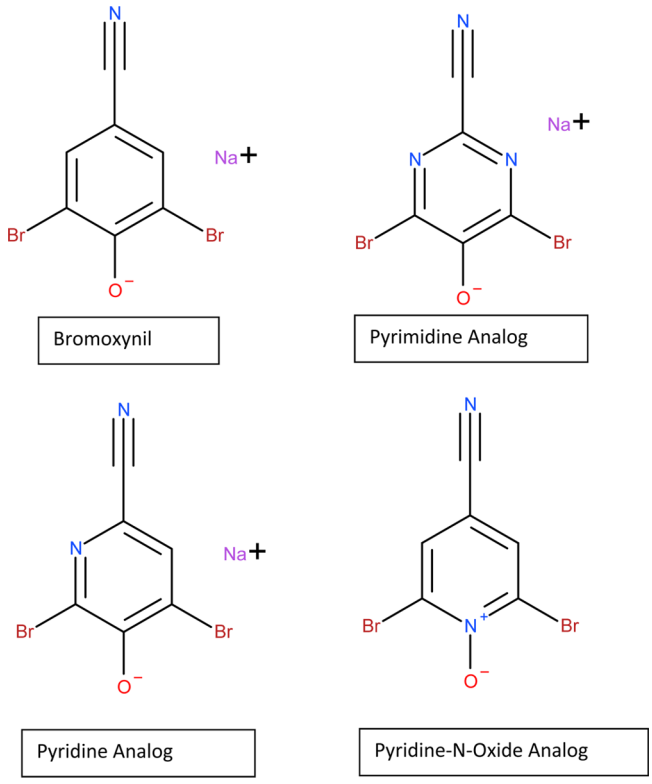

Figure 1. Chemical structures of bromoxynil and the heterocyclic analogues synthesized and tested at the University of Tennessee (Knoxville, TN, USA) during 2012 and 2013.

MATERIALS AND METHODS

Compound Synthesis (Figure 1). A 3,5-dibromo-4-hydroxybenzonitrile bromoxynil salt (bromoxynil, Figure 2) compound was synthesized following procedures from Gulbenk and Ruetman.[30] A total of 300 mg of 4-hydroxybenzonitrile, 1500 mg of sodium bromate, and 2050 mg of sodium bromide was dissolved in 15 mL of deionized water in a 250 mL round-bottom flask with a magnetic stir bar. Subsequently, the flask was capped with a rubber stopper and vented with a nitrogen balloon while 6 mL of concentrated hydrochloric acid (HCl) was slowly added to the reaction with a syringe over a period of 10 min. The flask was kept over a magnetic stir plate for 24 h at 20 °C. Finally, the solution was subjected to vacuum rotary evaporation

dx.doi.org/10.1021/jf404209d | J. Agric. Food Chem. 2014, 62, 329−336

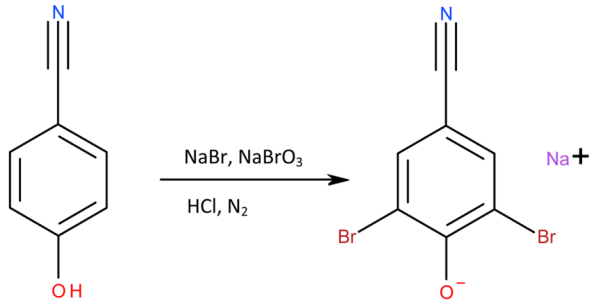

4-hydroxybenzonitrile

3-5 dibromo-4-hydroxy-benzonitrile (Bromoxynil)

Figure 2. Synthesis of 3,5-dibromo-4-hydroxybenzonitrile (bromoxynil) evaluated in greenhouse trials at the University of Tennessee (Knoxville, TN, USA) during 2012 and 2013.

(Buchi R-114. Nine Buchi Labortechnik AG, Flawil, Switzerland). Structural conformation was determined by direct analysis in real time (DART) HR mass spectrometry MS (m/z): 276.91 (found). A 2,4-dibromo-6-cyano-5-pyridin-3-olate sodium salt (pyridine) was also brominated using the same technique using 5-hydroxypyridine-2-carbonitrile starting material (pyridine; Figure 3). Structural

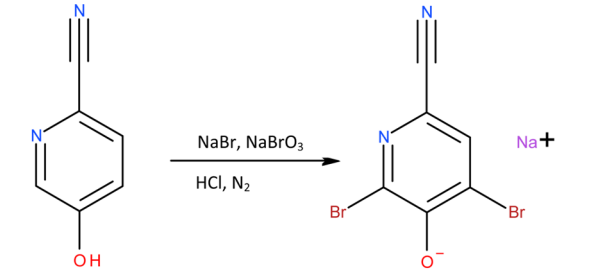

5-hydroxy-pyridine-2-carbonitrile

2,4-dibromo-6-cyano-5-pyridin-3-olate (Pyridine)

Figure 3. Synthesis of 2,4-dibromo-6-cyano-5-pyridin-3-olate (pyridine) evaluated in greenhouse trials at the University of Tennessee (Knoxville, TN, USA) during 2012 and 2013.

conformation was determined by DART HR mass spectrometry MS (m/z): 277.9 (found). However, because 5-hydroxypyridine-2-carbonitrile is more electrophilic than 4-hydroxybenzonitrile, fewer equivalencies of sodium bromate (753 mg) and sodium bromide (1028 mg) were required to make pyridine.

The first time step of the synthesis of 4,6-dibromo-2-cyanopyrimidin-5-olate sodium salt (pyrimidine; Figure 4) required 300 mg of 5-benzyloxypyrimidine-2-carbonitrile (Waterstone Techology, St. Carmel, IN, USA), which was dissolved in 20 mL of acetic acid and mixed with 30 mg of a 10% carbon palladium catalyst (Strem Chemicals, Newburyport, MA, USA) in a 250 mL round-bottom flask with a magnetic stir bar. Subsequently, the flask was capped and vented with hydrogen gas and reacted over a magnetic stir plate for 36 h at 20 °C. After 36 h, the solution was poured onto a Celite filter aid (Fisher Scientific, Fair Lawn, NJ, USA) covered Büchner funnel connected to an aspirator. The liquid phase was subjected to vacuum rotary evaporation and then dried under a high vacuum for 24 h. The structure of 5-hydroxypyrimidine-2-carbonitrile was confirmed by DART HR mass spectrometry (m/z): 121.1 (found). Next, 600 mg of sodium bromate and 900 mg of sodium bromide were dissolved in 15 mL of deionized water with 250 mg of 5-hydroxypyrimidine-2-carbonitrile in a 250 mL round-bottom flask with magnetic stir bar. Subsequently, the flask was capped with a rubber stopper and vented with a nitrogen balloon while 6 mL of HCl was slowly added to the reaction with a syringe over 10 min. The flask was kept over a magnetic stir plate for 24 h at 20 °C. The solution was then subjected to vacuum rotary evaporation. The structure of 4,6-dibromo-2-cyano-pyrimidin-5-olate sodium was confirmed by DART HR mass spectrometry MS (m/z): 278.89 (found).

Synthesis of 2,6-dibromo-1-oxidopyridin-1-ium-4-carbonitrile (pyridine-*N*-oxide; Figure 5) required a different bromination technique. Bromination of pyridine at the 2- and 6-positions within the ring structure of pyridine is difficult and requires drastic conditions that typically involve high pressure and vapor phase reactions at temperatures >500 °C.[24] However, displacement of chlorine with bromine at the 2,6-positions on pyridine had previously been performed under less drastic conditions.[31] To avoid vapor phase reactions, 213 mg of 2,6-dichloro-4-pyridinecarbonitrile was dissolved in 10 mL of acetic acid in a capped 250 mL three-neck round-bottom flask with a magnetic stir bar vented with a nitrogen balloon. The flask was attached to a condenser and an addition funnel in a hot oil bath at 103 °C over a magnetic stir plate. A total volume of 2 mL of hydrobromic acid was added to the solution through the addition funnel over a period of 5 min. After 9 h, 2.9 mL of phosphorus

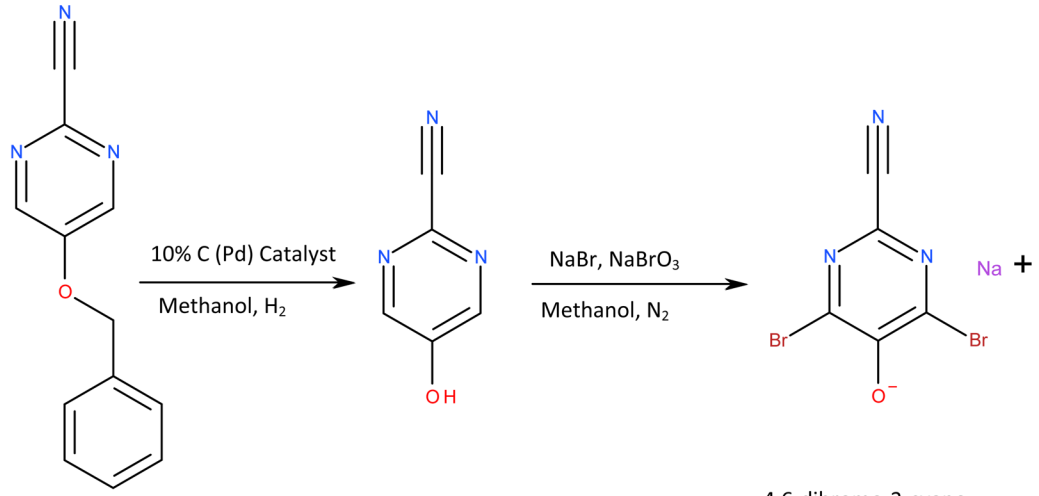

5-benzyloxypyrimidine-2-carbonitrile

5-hydroxy-pyrimidine-2-carbonitrile

4,6-dibromo-2-cyano-pyrimidin-5-olate

Figure 4. Synthesis of 4,6-dibromo-5-hydroxypyrimidine-2-carbonitrile (pyrimidine) evaluated in greenhouse trials at the University of Tennessee (Knoxville, TN, USA) during 2012 and 2013.

dx.doi.org/10.1021/jf404209d | *J. Agric. Food Chem.* 2014, 62, 329−336

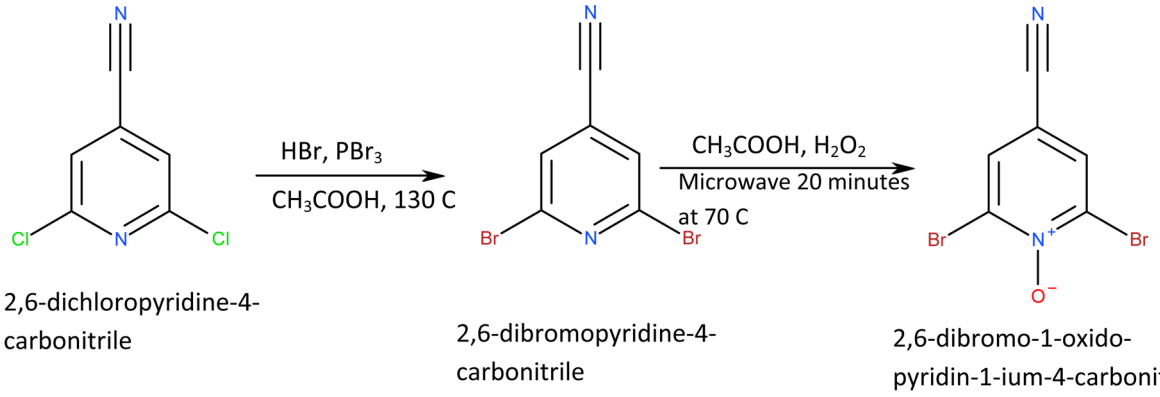

Figure 5. Synthesis of 2,6-dibromo-1-oxidopyridin-1-ium-4-carbonitrile (pyridine-*N*-oxide) evaluated in greenhouse trials at the University of Tennessee (Knoxville, TN, USA) during 2012 and 2013.

tribromide was added to the reaction with a syringe over 45 min and the reaction continued for an additional 16 h at 130 °C. The product of this reaction was a red solution that was cooled in an ice bath and diluted with 20 mL of dichloromethane and 40 mL of deionized water. The phases were mixed in a separation funnel, and the organic layer was extracted and subjected to vacuum rotary evaporation. The structure of the product, 2,6-dibromopyridine-4-carbonitrile, was confirmed through DART HR mass spectrometry MS (m/z): 272.5 (found). A total of 200 mg of 2,6-dibromopyridine-4-carbonitrile was then dissolved in 3 mL of glacial acetic acid and 1.5 mL of 30% hydrogen peroxide. The reaction mixture was exposed to 70 W of microwave irradiation for 20 min at normal absorption using a Biotage Initiator robot (Biotage, Kungsgatan, Sweden) following a protocol by Khrustalev et al.[32] Next, 15 mL of deionized water was added to the final solution and later removed using vacuum rotary evaporation. The product, 2,6-dibromo-1-oxidopyridin-1-ium-4-carbonitrile (pyridine-*N*-oxide), was confirmed using DART HR mass spectrometry MS (m/z): 277.6 (found).

All mass spectrometry analyses were conducted at the Mass Spectrometry Center located in the Department of Chemistry at the University of Tennessee. The DART analyses were performed using a JEOL AccuTOF-D time-of-flight (TOF) mass spectrometer with a DART ionization source from JEOL USA, Inc. (Peabody, MA, USA). Mass spectrometry solutions were prepared with methanol.

Weed and Crop Response Greenhouse Study. To evaluate the crop tolerance and weed control efficacy of synthesized bromoxynil analogues (bromoxynil, pyridine, pyrimidine, and pyridine-9*N*-oxide), an array of crops and weeds were propagated at the University of Tennessee Plant Science Greenhouse (Knoxville, TN, USA; 35.946471 latitude, 83.938558 longitude) including soybean, cotton, redroot pigweed, velvetleaf, large crabgrass, and pitted morningglory. All plants were grown in plastic 10.2 × 10.2 cm circular pots (Dillen Products/Myers Industries, Inc., Middlefield, OH, USA) containing peat-based growing media (ProMix BX Mycorrhizae, Premier Tech Horticulture, Quakertown, PA, USA) and treated 10 days after seeding. The experiment was conducted from Octboer 6 until 30, 2012, and repeated from November 14 until December 8, 2012. During both experimental runs the average air temperature in the climate-controlled greenhouse was 23 °C, whereas the lowest/highest air temperatures recorded were 20/30 °C. Mean daytime light levels during this period were 280 μmol m^{-2} s^{-1}. Irrigation was supplied through an overhead mist system and was withheld for 24 h after experimental herbicide application to ensure adequate time for foliar absorption of the experimental herbicides.

The compounds were applied POST at a rate of 0.28 kg ha^{-1}. This rate was chosen because it is the lowest labeled rate of bromoxynil recommended for weed control.[22] Additionally, the quantities of the analogues for use in studies were limited given that the yields of the aforementioned synthesis processes ranged from 20 to 35%. All compounds were dissolved in a mixture of acetone (3 mL) and deionized water (32 mL) and agitated using a (CL-18) sonicator (Fisher Scientific International Inc., Hampton, NH, USA) prior to application. Subsequently, the solutions were mixed with 0.1% nonionic surfactant. The solutions were then applied to the plants using an enclosed spray chamber (Generation III track sprayer; DeVries 10 Manufacturing, Hollandale, MN, USA) in deionized water carrier at 215 L ha^{-1} with an 8004 EVS nozzle (Teejet, Wheaton, IL, USA).

Visual percent plant injury ratings were recorded 7 days after treatment (DAT), whereas dry aboveground biomass was recorded 14 days after treatment. Aboveground biomass was harvested from every plant and oven-dried (Thelco 130D laboratory oven, Precision Scientific) at 65 °C for 3 days and weighed. Chlorophyll fluorescence (F_V/F_M) was recorded 10 DAT from soybean using a pulse-modulated fluorometer (OS1-FL, Opti-Sciences, Inc., Hudson, NH, USA).

Glyphosate Resistant Palmer Amaranth (*Amaranthus palmeri*) Greenhouse Study. A second study was conducted to evaluate bromoxynil, pyridine, pyrimidine, and pyridine-*N*-oxide for control of glyphosate-resistant Palmer amaranth (gift from Dr. Chad Brommer, BASF Research Triangle Park, NC, USA) from February 20 to March 13, 2013. Potting medium and irrigation conditions in the greenhouse were the same as previously described for the weed and crop response greenhouse study. The application rate in this study was increased to 0.56 kg ha^{-1} considering that these compounds imparted minimal injury to Palmer amaranth when applied at 0.28 kg ha^{-1} in prior experiments.

Statistical Analysis. All experiments were conducted in a completely randomized design (CRD) with three replications. All data were subjected to analysis of variance (ANOVA), and means were separated using Fisher's protected LSD at α = 0.05 in SAS (SAS Institute v. 9.2, Cary, NC, USA). Percent visual injury ratings were arscine transformed prior to analysis. Interpretations were not different from nontransformed data. Thus, nontransformed percent visual ratings are presented for clarity.

Docking Calculations. A crystal structure of the D1 and D2 proteins was extracted from the PSII complex of *Thermosynechococcus elongatus* at 2.9 Å resolution (Protein Data Bank entry 3BZ1)[33] and incorporated into the Molecular Operating Environment (MOE, 2012.10; Chemical Computing Group Inc., Montreal, QC, Canada) program. Structural optimization was performed on the Q_B binding site to include the nonheme iron, the four surrounding histidine ligands (D1-Hist$_{215}$, D1-His$_{272}$, D2-His$_{214}$, and D2-His$_{268}$), and the D1 residues of the QB binding site that consisted of Met$_{214}$, Leu$_{218}$, Val$_{219}$, Tyr$_{246}$, Ile$_{248}$, Ala $_{251}$, His$_{252}$, Phe$_{255}$, Ser$_{264}$, Phe$_{265}$, and Leu $_{271}$). The bromoxynil compounds were constructed in MOE; subsequently, Amber forcefield was used to optimize molecular mechanics.[34] Geometry optimization and energy minimization were applied to the system containing bromoxynil and the 3BZI protein. Bromoxynil was then inserted proximal to the binding pocket, and docking simulations were performed. Heterocyclic analogues were substituted for bromoxynil, and docking simulations were repeated with the analogues. To simulate physiological pH conditions, the CO group

dx.doi.org/10.1021/jf404209d | J. Agric. Food Chem. 2014, 62, 329−336

Table 1. Crop and Weed Species Injury 7 Days following Applications of Bromoxynil and the Heterocyclic Analogues of Bromoxynil at 0.28 kg ai ha^{-1}[a]

	injury[b,c] (%)					
treatment	soybean	cotton	pitted morningglory	redroot pigweed	velvetleaf	large crabgrass
bromoxynil	35 a	36 b	45 b	12 b	21 a	6 a
pyridine	41 a	16 c	45 b	30 a	11 a	9 a
pyrimidine	16 b	25 c	22 c	18 b	18 a	5 a
pyridine-*N*-oxide	45 a	38 b	55 a	33 a	25 a	13 a

[a]Means were combined from two runs of a greenhouse experiment conducted in Knoxville, TN, USA, in 2012. [b]Injury was evaluated visually on a 0 (no injury) to 100% (complete kill) scale relative to a nontreated check. [c]Means within the same column followed by the same letter are not significantly different according to Fisher's protected least significant difference test at the 0.05 level.

Table 2. Crop and Weed Species Aboveground Biomass 14 Days following Applications of Bromoxynil and the Heterocyclic Analogues of Bromoxynil at 0.28 kg ai ha^{-1}[a]

	aboveground biomass[b,c] (g per pot)					
treatment	soybean	cotton	pitted morningglory	redroot pigweed	velvetleaf	large crabgrass
bromoxynil	1.20 a	0.30 bc	0.95 b	0.24 ab	0.60 a	0.36 b
pyridine	0.92 b	0.21 c	0.79 bc	0.18 b	0.45 bc	0.26 b
pyrimidine	1.18 a	0.4 b	0.90 b	0.23 ab	0.46 bc	0.30 b
pyridine-*N*-oxide	0.84 b	0.19 c	0.35 e	0.10 c	0.48 bc	0.25 b
nontreated	1.33 a	0.68 a	1.30 a	0.25 a	0.62 a	0.50 a

[a]Means were combined from two runs of a greenhouse experiment conducted in Knoxville, TN, USA, in 2012. [b]Means within a column followed by the same letter are not significantly different according to Fisher's protected least significant difference test at the 0.05 level. [c]Above ground biomass was harvested from every plant and oven-dried at 65 °C for 3 days and weighed.

from all compounds was deprotonated. The simulation distance between herbicide and target amino acids in the binding pocket was transcribed in Symx Draw (version 4.0, Accelrys Inc., San Diego, CA, USA) to enhance visual clarity.

RESULTS AND DISCUSSION

Weed and Crop Response. No treatment-by-experimental run interactions were detected in percent injury or aboveground biomass data; therefore, data from both runs were combined.

Application of bromoxynil resulted in >35% injury to soybean, cotton, and pitted morningglory (Table 1). However, when bromoxynil was applied to velvetleaf, redroot pigweed, or large crabgrass, injury measured <25% (Table 1).

Different trends were observed with applications of heterocyclic bromoxynil analogues. Applications of the pyridines (pyridine and pyridine-*N*-oxide) generally injured all plant species more than pyrimidine. Injury ratings were similar when pyridine and pyridine-*N*-oxide were compared; however, applications of pyridine-*N*-oxide resulted in more injury to pitted morningglory and cotton than pyridine (Table 1). This response was especially pronounced following treatment to cotton, where application of pyridine-*N*-oxide resulted in 38% injury whereas application of pyridine resulted in only 16% injury. Interestingly, pyridine and pyridine-*N*-oxide were also more injurious to redroot pigweed when compared to bromoxynil. None of the herbicides injured large crabgrass >13%.

Generally, aboveground biomass data supported visual assessments of plant injury (Table 2). However, pyridine reduced velvetleaf aboveground biomass more than bromoxynil, which caused greater visual injury than pyridine. Technical grade material was applied in our research, and volatility in the spray chamber may have limited the effectiveness of the compound. Commercially formulated herbicides often have emulsifiers, detergents, wetting agents, and other surfactants that improve herbicide efficacy.[35]

Pyridine reduced photosynthetic efficiency more than any other treatment (Table 3.). Analysis of F_V/F_M data did not always correlate with visual ratings. For example, pyridine reduced PSII efficiency significantly more than pyridine-*N*-oxide; however, pyridine-*N*-oxide generally induced more phytotoxicity than pyridine (Tables 2 and 3). Pyrimidine did not reduce F_V/F_M significantly more than the nontreated check.

Table 3. Impact of Compounds Applied to Soybeans at 0.28 kg ai ha^{-1} on F_V/F_M Values Taken 10 Days after Treatment

treatment	F_V/F_M[a]
bromoxynil	0.456 b
pyridine	0.222 c
pyrimidine	0.671 a
pyridine-*N*-oxide	0.456 b
nontreated	0.804 a

[a]Means within a column followed by the same letter are not significantly different according to Fisher's protected least significant difference test at the 0.05 level.

The most interesting trend observed in the weed and crop response study was the ability of the pyridine analogues (pyridine and pyridine-*N*-oxide) to inflict greater phytotoxicity on redroot pigweed than bromoxynil. Although the redroot pigweed injury observed in this study would not be considered acceptable, the potential impact on weed management that the pyridine herbicides would have when applied as a formulated product at higher rates is intriguing.

Glyphosate-Resistant Palmer Amaranth Study. Applications of bromoxynil and pyridine all injured glyphosate-resistant Palmer amaranth >80% (Table 4). Although it cannot be determined statistically, it appeared that doubling the application rate to 0.56 kg ha^{-1} in this study greatly improved

Table 4. Glyphosate-Resistant Palmer Amaranth (*Amaranthus palmeri*) Injury and Aboveground Biomass following Applications of Bromoxynil and the Heterocyclic Analogues of Bromoxynil at 0.56 kg ai ha^{-1} in a Greenhouse Experiment Conducted in Knoxville, TN, USA, in 2013[a]

treatment	injury[b,c] (%)	aboveground biomass[c,d]
bromoxynil	87 a	0.18 cd
pyridine	83 a	0.08 d
pyrimidine	25 b	0.41 b
pyridine-*N*-oxide	25 b	0.30 bc
nontreated		0.80 a

[a]Injury and aboveground biomass data were collected 7 and 14 days after treatment, respectively. [b]Injury was evaluated visually on a 0 (no injury) to 100% (complete kill) scale relative to the nontreated check. [c]Means within a column followed by the same letter are not significantly different according to Fisher's protected least significant difference test at the 0.05 level. [d]Aboveground biomass was harvested from every plant and oven-dried at 65 C for 3 days and weighed.

the efficacy of bromoxynil and pyridine against pigweed species. Application of pyrimidine and pyridine-*N*-oxide injured glyphosate-resistant Palmer amaranth ~25%. This response was surprising considering the level of redroot pigweed injury observed with pyridine-*N*-oxide in the weed and crop tolerance study (Table 1). Whereas pyridine-*N*-oxide reduced glyphosate-resistant Palmer amaranth aboveground biomass more than pyrimidine, reductions in aboveground biomass were less than with bromoxynil and pyridine (Table 4). Glyphosate-resistant Palmer amaranth biotypes typically exhibit increased transcription of EPSP-synthase.[36] Therefore, increased expression of cytochrome-P450s, glutathione-*S*-transferases, and altered ABC-transporters in Palmer amaranth are likely not responsible for the decreased effectiveness of pyridine-*N*-oxide in this study.

Docking Simulations. Bromoxynil docking in our research was similar to work done by Takahashi et al.[16] Interestingly, the distance of the hydrogen bond between the CO group from the pyridine and the D1 His_{215} was closer than was observed with bromoxynil (Figure 6). This may explain why pyridine performed better than bromoxynil in the weed and crop response study. However, pyridine is supposedly less injurious to broadleaf crops as described by Gullbenk and Ruetman.[30] The decreased susceptibility of broadleaf crops to pyridine may be due to metabolism. The pyrimidine analogue was inverted in the binding pocket relative to the other compounds tested, and the CN group formed a hydrogen bond with His_{215} during the simulation. Hydrogen bonding with a CN group is typically weaker when compared to a CO group; additionally, the bond distance was greater in the pyrimidine simulation than in the pyridine simulation. This could explain why pyridine resulted in more injury than pyrimidine during our greenhouse trials. Pyrimidine did not form a strong hydrogen bond with His_{215}. Different parameters likely need to be applied to the environment to account for the unique properties of a pyridine-*N*-oxide bromoxynil analogue. An alternative simulation performed with pyridine-*N*-oxide showed that the oxyanion interacted with the hydrogen backbone of His_{215} as opposed to the imidazole ring. Additionally, a hydrogen bond formed between the ring of pyridine-*N*-oxide and the sulfur atom on Met_{214}. The presence of a cation at the QB binding site may influence the π electron system of the Q_A–His_{214}–Iron–His_{215}–Q_B bridge, which is interesting information that could be used to design future compounds.

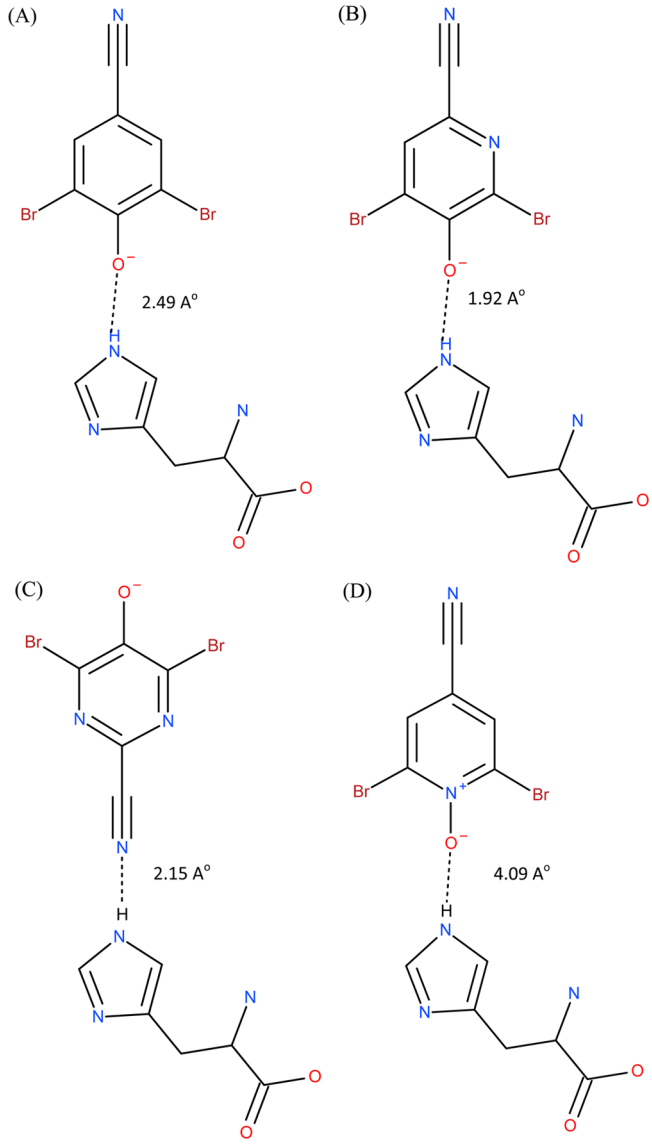

Figure 6. Docking simulations of bromoxynil and heterocyclic analogues (A) bromoxynil, (B) pyridine, (C) pyrimidine, and (D) pyridine-*N*-oxide. The hydrogen bond distance between the ligand and $histidine_{215}$ is in angstroms (A°).

Structure–Activity Relationship. The primary metabolite of bromoxynil in nonsusceptible plants and microbial soil systems results from the hydrolysis of the nitrile group to a carboxylic acid or amide.[37,38] Additionally, replacement of the bromines with hydroxyl groups results in a less herbicidal metabolite.[8,37] This hydroxylation reaction involves the formation of a hydroxide anion, which then initiates an S_N2 reaction by attacking the meta-positioned carbons on bromoxynil. An electron pair is then donated to bromine, which leaves the ring and forms a Br^- ion. Pyridine and pyrimidine analogues are less electron dense compared to bromoxynil and would be more susceptible to hydroxylation and other nucleophilic attacks. If hydroxylation of bromine is the metabolic mechanism that results in decreased efficacy of bromoxynil, then pyrimidine would be the most readily metabolized analogue tested because it is the most electrophilic. This theory is supported by the results of the greenhouse trials as well as what was observed in the docking calculations. Pyrimidine did not bind as strongly to His_{215} in the binding

dx.doi.org/10.1021/jf404209d | J. Agric. Food Chem. 2014, 62, 329–336

pocket as bromoxynil or pyridine and is likely easier to metabolize, thus reducing weed and crop injury. Pyridine formed a stronger hydrogen bond with His_{215} in the binding pocket compared to bromoxynil; however, it is likely metabolized more easily than bromoxynil, and thus did not significantly injure all plants more than bromoxynil. As mentioned earlier, the pyridine-*N*-oxide analogue is similar to bromoxynil with regard to electrophilicity and therefore may not be as easily hydroxylated as the pyridine and pyrimidine analogues. Interestingly, application of pyridine-*N*-oxide resulted in greater redroot pigweed control than bromoxynil with less damage to cotton and soybean. Alternatively, the structure of pyridine-*N*-oxide may be altered by metabolism in both crop and weed species, resulting in greater herbicidal activity. This scenario could be possible because the docking simulations indicated that pyridine-*N*-oxide hydrogen bond distance with His_{215} was not optimal.

Evaluating the stability of pyridine-*N*-oxide, synthesizing ester analogues of pyridine and pyrimidine, and optimizing formulations for all of these compounds would be important for further characterizing the potential of these heterocyclic bromoxynil analogues as new herbicides. The ability of the nonformulated pyridine herbicides to inflict significant damage to multiple weed species necessitates evaluating these compounds within multiple formulations. Additionally, evaluating the safety of the heterocyclic compounds on *bxn* crops would be of interest. The *bxn* trait consists of a nitrilase gene that detoxifies bromoxynil by converting the nitrile group into a carboxylic acid.[39] Cotton containing this trait may be safely sprayed with bromoxynil. The effectiveness of pyridine on glyphosate-resistant Palmer amaranth and the potential safety of the compounds in *bxn* plants may provide a new tool for farmers to manage cropping systems where glyphosate-resistant weeds are problematic.

AUTHOR INFORMATION

Present Address

[¶](M.A.C.) Syngenta Crop Protection, Vero Beach, Florida 32967.

Notes

The authors declare no competing financial interest.

REFERENCES

(1) Duke, S. O. Why have no new herbicide modes of action appeared in recent years? *Pest Manag. Sci.* **2011**, *68*, 505−512.

(2) Heap I. M., The international survey of herbicide-resistant weeds; available at http://www.weedscience.org/in.asp (accessed May 9, 2013).

(3) Witschel, M.; Rohl, F.; Niggeweg, R.; Newton, T. In search of new herbicidal inhibitors of the non-mevalonate pathway. *Pest Manag. Sci.* **2013**, *69*, 559−563.

(4) Grossman, K.; Christiansen, N.; Looser, R.; Tresch, S.; Hutzler, J.; Pollmannc, S.; Ehrhardt, T. Physionomics and metabolomics − two key approaches in herbicidal mode of action discovery. *Pest Manag. Sci.* **2012**, *68*, 494−504.

(5) Rutherford, A. W.; Krieger-Liszkay, A. Herbicide-induced oxidative stress in photosystem II. *Trends Biochem. Sci.* **2001**, *26*, 648−653.

(6) Diner, B. A.; Schlodder, E.; Nixon, P. J.; Coleman, W. J.; Rappaport, F.; Lavergne, J.; Vermaas, W. F. J.; Chisholm, D. A. Site-directed mutations at D1-His_{198} and D2-His_{197} of photosystem II in *Synechocystis* PCC 6803: sites of primary charge separation and cation and triplet stabilization. *Biochemistry* **2001**, *40*, 9265−9281.

(7) Diner, B. A.; Babcock, G. T. Structure, dynamics, and energy conversion efficiency in photosystem II. In *Oxygenic Photosynthesis: The Light Reactions*; Ort, D., Yocum, C. F., Eds.; Kluwer Academic Publishers: Dordrecht, The Netherlands, 1996; pp 213−247.

(8) Debus, R. J. Amino acid residues that modulate the properties of tyrosine YZ and the manganese cluster in the water oxidizing complex of photosystem II. *Biochim. Biophys. Acta* **2001**, *1503*, 164−176.

(9) Diner, B. A. Amino acid residues involved in the coordination and assembly of the manganese cluster of photosystem II. Proton-coupled electron transport of the redox-active tyrosines and its relationship to water oxidation. *Biochim. Biophys. Acta* **2001**, *1503*, 147−163.

(10) Oettmeier, W. Herbicide resistance and supersensitivity in photosystem II. *Cell. Mol. Life Sci.* **1999**, *55*, 1255−1277.

(11) Trebst, A. Inhibitors in the functional dissection of the photosynthetic electron transport system. *Photosynth. Res.* **2007**, *92*, 217−224.

(12) Trebst, A. The molecular basis of plant resistance to photosystem II herbicides. In *Molecular Genetics and Evolution of Pesticide Resistance*; Brown, T. M., Ed.; ACS Symposium Series 645; American Chemical Society: Washington, DC, 1996; pp 44−51.

(13) Trebst, A. The three-dimensional structure of the herbicide binding niche on the reaction center polypeptides of photosystem II. *Z. Naturforsch.* **1987**, *C42*, 742−750.

(14) Wraight, C. A. Oxidation−reduction physical chemistry of the acceptor quinone complex in bacterial photosynthetic reaction centers: evidence for a new model of herbicide activity. *Isr. J. Chem.* **1981**, *21*, 349−354.

(15) Ido, K.; Gross, C. M.; Guerrero, F.; Sedoud, A.; Lai, T.; Ifuku, K.; Rutherford, A. W.; Krieger-Liszkay, A. High and low potential forms of the QA quinone electron acceptor in photosystem-II of *Thermosynechococcus elongatus* and spinach. *J. Photochem. Photobiol. B: Biol.* **2011**, *104*, 154−157.

(16) Takahashi, R.; Hasegawa, K.; Takano, A.; Noguchi, T. Structures and binding sites of phenolic herbicides in the Q_B pocket of photosystem II. *Biochemistry* **2010**, *49*, 5445−5454.

(17) Devine, M. D.; Shukla, A. Altered target sites as a mechanism of herbicide resistance. *Crop Prot.* **2000**, *19*, 881−889.

(18) Gronwald, J. W. Resistance to photosystem II inhibiting herbicides. In *Herbicide Resistance in Plants: Biology and Biochemistry*; Powles, S. B., Holtum, J. A. M., Eds.; CRC Press: Boca Raton, FL, USA, 1994; pp *27*−60.

(19) Van Oorschot, J. L.; Van Leeuwen, P. H. Inhibition of photosynthesis in intact plants of biotypes resistant or susceptible to atrazine and cross-resistant to other herbicides. *Weed Res.* **1988**, *28*, 223−230.

(20) Gressel, .J Why get resistance? It can be prevented or delayed. In *Herbicide Resistance in Weeds and Crops*; Caseley, J. C., Cussans, G. W., Atkin, R. K., Eds.; Butterworth-Heinemann: Oxford, UK, 1991; pp 1−26.

(21) Carpenter, K.; Cottrell, H. J.; De Silva, W. H.; Heywood, B. J.; Leeds, W. G.; Rivett, K. F.; Soundy, M. L. Chemical and biological properties of two new herbicides − ioxynil and bromoxynil. *Weed Res.* **1964**, *4*, 175−195.

(22) Senseman, S. A., Ed. *Herbicide Handbook*, 9th ed.; Weed Science Society of America: Lawrence, KS, USA, xxxx; p 22.

(23) Takano, A.; Takahashi, R.; Suzuki, H.; Noguchi, T. Herbicide effect on the hydrogen-bonding interaction of the primary quinone electron acceptor QA in photosystem II as studied by Fourier transform infrared spectroscopy. *Photosynth. Res.* **2008**, *98*, 159−167.

(24) Katritzky, A. R.; Ramsden, C. A.; Joule, J. A.; Zhdankin, V. V. *Handbook of Heterocyclic Chemistry*, 3rd ed.; Oxford, UK, 2010.

(25) Patterson, M. G.; Norris, B. E. Transgenic cotton allows over-the top weed control. In *Highlights of Agricultural Research*; Alabama Agricultural Experiment Station, Auburn University: Auburn, AL, USA, 1993; Vol. 40, p 13.

(26) Smith, M. C.; Jordan, D. L.; Frans, R. E.; McClelland, M. R. Influence of application rate and timing on efficacy of bromoxynil. *Proc. Beltwide Cotton Conf.* **1993**, *17*, 1519.

(27) Eberlein, C. V.; Guttieri, M. J.; Steffen-Campbell, J. Bromoxynil resistance in transgenic potato clones expressing the *bxn* gene. *Weed Sci.* **1998**, *46*, 150−157.
(28) Gentsch, B. J.; Weber, J. B. Absorption and translocation of bromoxynil following application to roots, stems, and leaves of two *Ipomoea* spp. *Abstr. Weed Sci. Soc. Am.* **1986**, *26*, 19.
(29) Boydston, R. A.; Al-Khatib, K. Efficacy, site of uptake, and retention of bromoxynil in common lambsquarters with conventional and sprinkler application. *Weed Sci.* **1993**, *41*, 166−171.
(30) Gulbenk, A. H.; Ruetman, S. H. (Dow Chemical Co.) U.S. Patent 3,956,338, 1975.
(31) McKendry, L. H. Synthesis of a substituted cyclopropanecurboxylate. *J. Labelled Compd. Radiopharm.* **1984**, *21*, 401−408.
(32) Khrustalev, D. P.; Khamzina, G. T.; Fazylov, S. D.; Muldakhmetov, Z. M. Microwave activation in the synthesis of nitrogen heterocycles, *N*-oxides of pyridine series. *Russ. J. Gen. Chem.* **2008**, *78*, 1577−1578.
(33) Guskov, A.; Kern, J.; Gabdulkhakov, A.; Broser, M.; Zouni, A.; Saenger, W. Cyanobacterial photosystem II at 2.9-Å resolution and the role of quinones, lipids, channels and chloride. *Nat. Struct. Mol. Biol.* **2009**, *16*, 334−342.
(34) Hornak, V.; Abel, R.; Okur, A.; Strockbine, B.; Roitberg, A.; Simmerling, C. Comparison of multiple Amber force fields and development of improved protein backbone parameters. *Proteins* **2006**, *65*, 712−725.
(35) Behrens, R. W. The physical and chemical properties of surfactants and their effects on formulated herbicides. *Weeds* **1964**, *12*, 255−258.
(36) Gaines, T. A.; Shaner, D. L.; Ward, S. M.; Leach, J. E.; Preston, C.; Westra, P. Mechanism of resistance of evolved glyphosate-resistant Palmer amaranth (*Amaranthus palmeri*). *J. Agric. Food Chem.* **2011**, *59*, 5886−5889.
(37) Buckland, J. F.; Collins, R. F.; Pullin, E. M. Metabolism of bromoxynil octanoate in growing wheat. *Pest Manag. Sci.* **1973**, *4*, 149−162.
(38) Graß, B.; Mayer, H.; Nolte, J.; Preuß, G.; Zullei-Seibert, N. Studies on the metabolism of hydroxybenzonitrile herbicides: I. Mass spectrometric identification. *Pest Manag. Sci.* **2000**, *56*, 49−59.
(39) Stalker, D. M.; McBride, K. E.; Malyj, L. D. Herbicide-resistance in transgenic plants expressing a bacterial detoxification gene. *Science* **1988**, *242*, 419−423.